Supplementary Information: An algebraic non-equilibrium turbulence model of the high Reynolds number transition region

Nils T. Basse[a]

[a] *Independent Scientist*
Trubadurens väg 8, 423 41 Torslanda, Sweden

September 11, 2023

Abstract

This Supplementary Information document contains details of the algebraic turbulence model which have been omitted from the paper.

1. Introduction

This Supplementary Information (SI) document accompanies the paper [1]. It provides background information on the ingredients of the algebraic turbulence model discussed in the paper.

The SI is organised as follows: In Section 2, we describe the basic model. The turbulent viscosity ratio is discussed in Section 3, mixing length scales are covered in Section 4 and turbulence intensity definitions are presented in Section 5. Model input, assumptions and choices can be found in Sections 6, 7 and 8, respectively.

2. Basic model

We follow the treatment and nomenclature in [2], along with inspiration from [3].

For simplicity of exposition we treat simple shear flow, where the turbulent (eddy) viscosity (ν_t) hypothesis [4] can be written:

$$-\overline{uv} = \nu_t \times \mathcal{S}, \tag{S1}$$

Email address: nils.basse@npb.dk (Nils T. Basse)

with $-\overline{uv}$ being the Reynolds (shear) stress of the streamwise fluctuating velocity u and the wall-normal fluctuating velocity v. The mean shear rate (mean velocity gradient) is given by:

$$\mathcal{S} = \partial U/\partial z, \tag{S2}$$

which can be inverted to define a mean shear time scale:

$$\tau_{\mathcal{S}} = \frac{1}{\mathcal{S}} \tag{S3}$$

The turbulence production rate is:

$$\mathcal{P} = -\overline{uv} \times \mathcal{S} = \nu_t \times \mathcal{S}^2, \tag{S4}$$

where the turbulent viscosity is modelled as a product of characteristic length and velocity scales:

$$\nu_t = \ell^* \times u^* \tag{S5}$$

As a characteristic length scale we use the mixing length ℓ_m which will be defined in more detail in Section 4:

$$\ell^* = \ell_m \tag{S6}$$

Regarding the characteristic velocity scale, we treat the one originally proposed in Section 2.1 for reference. In the remainder of the paper we will use the modified characteristic velocity scale introduced in Section 2.2.

2.1. Original u^*

The characteristic velocity for the original mixing length hypothesis [5, 6] is:

$$u^* = u_{\mathrm{P}} = \ell_m |\mathcal{S}|, \tag{S7}$$

where we use the subscript "P" for Prandtl. This characteristic velocity and Equations (S5) and (S6) lead to a turbulent viscosity of:

$$\nu_t = \nu_{t,\mathrm{P}} = \ell_m \times \ell_m |\mathcal{S}| = \ell_m^2 |\mathcal{S}|, \tag{S8}$$

and, finally, by use of Equation (S1), an expression for the Reynolds stress:

$$-\overline{uv} = -\overline{uv}_{\mathrm{P}} = \nu_t \times \mathcal{S} = \ell_m^2 \mathcal{S}|\mathcal{S}| \tag{S9}$$

2.2. Modified u^*

Kolmogorov [7] and Prandtl [8] independently proposed the Kolmogorov-Prandtl velocity scale:

$$u^* = u_{\mathrm{K-P}} = c\sqrt{k}, \tag{S10}$$

where the subscript "K-P" is for Kolmogorov-Prandtl, c is a constant (but turns out to be a variable for our model) to be determined and k is the turbulent kinetic energy (TKE). Now, we define the turbulent viscosity as the product of the mixing length and the Kolmogorov-Prandtl velocity scale:

$$\nu_t = \nu_{t,\mathrm{K-P}} = \ell_m \times c\sqrt{k} \tag{S11}$$

Taylor proposed [9, 10] that the dissipation rate ε of the TKE can be written in this form:

$$\varepsilon = \frac{u^{*3}}{\ell^*}, \tag{S12}$$

and combining this expression with Equations (S6) and (S10) we arrive at:

$$\varepsilon = \frac{(c\sqrt{k})^3}{\ell_m} = \frac{C_D k^{3/2}}{\ell_m}, \tag{S13}$$

where $C_D = c^3$ and using Equations (S11) and (S13) the turbulent viscosity becomes:

$$\nu_t = cC_D \times \frac{k^2}{\varepsilon} = C_\mu \times \frac{k^2}{\varepsilon}, \tag{S14}$$

with $C_\mu = c^4$. Now we are able to introduce an expression for the turbulent production-to-dissipation ratio based on Equations (S4) and (S13):

$$\frac{\mathcal{P}}{\varepsilon} = \frac{\ell_m^2 \times c\sqrt{k} \times \mathcal{S}^2}{C_D k^{3/2}} = \frac{\ell_m^2 \times \mathcal{S}^2}{c^2 k}, \tag{S15}$$

which can be rearranged to:

$$c\sqrt{k} = \ell_m |\mathcal{S}| \left(\frac{\mathcal{P}}{\varepsilon}\right)^{-1/2} \tag{S16}$$

Comparing the equations in Section 2.1 with the equations in this section, we can write the Kolgomorov-Prandtl expressions as the Prandtl equations divided by $\sqrt{\mathcal{P}/\varepsilon}$:

$$u_{\mathrm{K-P}} = \ell_m |\mathcal{S}| \left(\frac{\mathcal{P}}{\varepsilon}\right)^{-1/2} = u_{\mathrm{P}} \left(\frac{\mathcal{P}}{\varepsilon}\right)^{-1/2} \tag{S17}$$

$$\nu_{t,\mathrm{K-P}} = \ell_m^2 |\mathcal{S}| \left(\frac{\mathcal{P}}{\varepsilon}\right)^{-1/2} = \nu_{t,\mathrm{P}} \left(\frac{\mathcal{P}}{\varepsilon}\right)^{-1/2} \tag{S18}$$

$$-\overline{uv} = -\overline{uv}_{\mathrm{K-P}} = \ell_m^2 \mathcal{S}|\mathcal{S}| \left(\frac{\mathcal{P}}{\varepsilon}\right)^{-1/2} = -\overline{uv}_{\mathrm{P}} \left(\frac{\mathcal{P}}{\varepsilon}\right)^{-1/2} \tag{S19}$$

So a production-to-dissipation ratio above one implies lower velocity, turbulent viscosity and Reynolds stress compared to the original Prandtl formulation.

2.3. Derived quantities

Manipulating the equations in Section 2.2, we can reformulate the expressions to establish alternative dependencies explicitly.

The TKE production rate can be written using Equations (S13), (S15) and (S16):

$$\mathcal{P} = \ell_m^2 |\mathcal{S}|^3 \left(\frac{\mathcal{P}}{\varepsilon}\right)^{-1/2}, \tag{S20}$$

while c, C_D and C_μ can be expressed in terms of the TKE, the mixing length, the mean shear rate and the TKE production-to-dissipation ratio using Equation (S16):

$$c = \frac{\ell_m |\mathcal{S}|}{\sqrt{k}} \left(\frac{\mathcal{P}}{\varepsilon}\right)^{-1/2} \tag{S21}$$

$$C_D = c^3 = \frac{\ell_m^3 |\mathcal{S}|^3}{k^{3/2}} \left(\frac{\mathcal{P}}{\varepsilon}\right)^{-3/2} \tag{S22}$$

$$C_\mu = c^4 = \frac{\ell_m^4 \mathcal{S}^4}{k^2} \left(\frac{\mathcal{P}}{\varepsilon}\right)^{-2} \tag{S23}$$

The TKE can be written explicitly from Equation (S16)

$$k = \frac{\ell_m^2 \mathcal{S}^2}{c^2} \left(\frac{\mathcal{P}}{\varepsilon}\right)^{-1}, \tag{S24}$$

and the TKE dissipation rate from Equations (S13) and (S16):

$$\varepsilon = \ell_m^2 |\mathcal{S}|^3 \left(\frac{\mathcal{P}}{\varepsilon}\right)^{-3/2} \tag{S25}$$

The ratio of the absolute value of the Reynolds stress to the TKE can be written using Equation (S19) as:

$$\frac{|\overline{uv}|}{k} = \frac{\ell_m^2 \mathcal{S}^2}{k} \left(\frac{\mathcal{P}}{\varepsilon}\right)^{-1/2}, \tag{S26}$$

or - using Equations (S1) and (S14) - as:

$$\frac{|\overline{uv}|}{k} = \frac{\nu_t \mathcal{S}}{k} = \frac{\mathcal{S}}{k} C_\mu \frac{k^2}{\varepsilon} = C_\mu \frac{\mathcal{S} k}{\varepsilon} \tag{S27}$$

The TKE production-to-dissipation ratio can be derived from Equations (S4) and (S14):

$$\frac{\mathcal{P}}{\varepsilon} = \frac{\nu_t \mathcal{S}^2}{\varepsilon} = \frac{\mathcal{S}^2}{\varepsilon} C_\mu \frac{k^2}{\varepsilon} = C_\mu \left(\frac{\mathcal{S} k}{\varepsilon}\right)^2 \tag{S28}$$

Combining Equations (S27) and (S28) we can also write the ratio of the absolute value of the Reynolds stress to the TKE as:

$$\frac{|\overline{uv}|}{k} = \left(C_\mu \frac{\mathcal{P}}{\varepsilon}\right)^{1/2} \tag{S29}$$

This last equation could also have been derived from Equations (S23) and (S26).

2.4. General formulation

Several quantities can be derived from k and ε and most will be used later in the paper. The first is a length scale where we use Equation (S13):

$$L = \frac{k^{3/2}}{\varepsilon} = \frac{\ell_m}{C_D}, \tag{S30}$$

and the corresponding ratio between the mixing length and this new length scale can be found using C_μ from Equation (S23):

$$\frac{\ell_m}{L} = c^3 = C_\mu^{3/4} = \frac{\ell_m^3 |\mathcal{S}|^3}{k^{3/2}} \left(\frac{\mathcal{P}}{\varepsilon}\right)^{-3/2} \tag{S31}$$

The second quantity is a turbulent time scale where we use Equations (S13) and (S27):

$$\tau_L = \frac{k}{\varepsilon} = \frac{|\overline{uv}|}{k} \frac{1}{C_\mu \mathcal{S}} = \frac{\ell_m}{C_D \sqrt{k}} = \frac{L}{\sqrt{k}} \tag{S32}$$

Note that in conjunction with Equation (S3), this time scale can be used to express a turbulence-to-mean shear time scale ratio:

$$\frac{\mathcal{S}k}{\varepsilon} = \frac{\tau_L}{\tau_\mathcal{S}} \tag{S33}$$

A frequency scale can be defined as a third quantity which is the inverse of the turbulent time scale:

$$\omega_L = \frac{\varepsilon}{k} = \frac{k}{|\overline{uv}|} C_\mu \mathcal{S} = \frac{C_D \sqrt{k}}{\ell_m} = \frac{\sqrt{k}}{L} \tag{S34}$$

Two-equation turbulence models can for example solve equations for k and ε ($k - \varepsilon$ [11]) or k and ω_L ($k - \omega_L$ [10]).

As the final, fourth, quantity we define the turbulent viscosity scale based on the length scale L:

$$\nu_{t,L} = \frac{k^2}{\varepsilon} = \frac{|\overline{uv}|}{C_\mu \mathcal{S}} = \frac{\ell_m \sqrt{k}}{C_D} = \sqrt{k} L \tag{S35}$$

2.5. Standard turbulence model constant C_μ

For standard turbulent viscosity models, [12] is used for the ratio of the absolute value of the Reynolds stress to the TKE:

$$\frac{|\overline{uv}|}{k} \approx 0.3 \tag{S36}$$

Along with an assumption of equilibrium flow:

$$\mathcal{P} \approx \varepsilon, \tag{S37}$$

we can use Equation (S29) to derive the standard turbulence model constant C_μ:

$$C_{\mu,\mathrm{B}} = (0.3)^2 = 0.09, \tag{S38}$$

where we use the subscript "B" for Bradshaw et al. [12].

As we have seen in Section 2.3 (Equation (S23)), we predict that C_μ scales with $(\mathcal{P}/\varepsilon)^{-2}$ for non-equilibrium flows.

We note that with the assumptions above, the turbulence-to-mean shear time scale ratio is:

$$\frac{\tau_L}{\tau_\mathcal{S}} = \frac{\mathcal{S}k}{\varepsilon} = \frac{|\overline{uv}|}{k}\frac{1}{C_{\mu,\mathrm{B}}} = \frac{10}{3}, \tag{S39}$$

where we have used Equations (S27) and (S33).

3. Turbulent Viscosity Ratio

We define the total viscosity as the sum of the kinematic (physical property) and turbulent (flow property) viscosity:

$$\nu_\mathrm{tot} = \nu_\mathrm{kin} + \nu_t \tag{S40}$$

From the two parts of the total viscosity we can calculate the turbulent viscosity ratio:

$$\nu_r = \frac{\nu_t}{\nu_\mathrm{kin}}, \tag{S41}$$

which is a quantity often used for inlet boundary conditions in CFD simulations, a typical default value being 10 [13].

The turbulence Reynolds number [2] is given as:

$$Re_L = \frac{\sqrt{k}L}{\nu_{\text{kin}}} = \frac{k^2}{\varepsilon\nu_{\text{kin}}}, \tag{S42}$$

where we have used Equation (S35). This means that the turbulent viscosity ratio can be written as the following product:

$$\nu_r = \frac{C_\mu \times \frac{k^2}{\varepsilon}}{\nu_{\text{kin}}} = C_\mu \times Re_L \tag{S43}$$

4. Turbulent Mixing Length Scales

4.1. von Kármán number

Before explicitly documenting the mixing length scales considered, we take a look at the variation of the global von Kármán number, which is derived by assuming that the streamwise mean velocity is given by the log-law across the entire flow. For the Superpipe measurements, a solution to this equation is given as "Solution 2" (see [14] for details) for smooth and rough wall pipe flow in Figure S1. In [14], we used a power-law fit to the smooth pipe data, but here we show that the measurements can equally well be described by a hyperbolic tangent function:

$$\kappa_g(Re_\tau) = -1.18 + 1.52 \times \tanh(2.15 \times 10^{-4} \times (Re_\tau + 8785.94)), \tag{S44}$$

with asymptotic limits:

$$\lim_{Re_\tau \to 0} \kappa_g(Re_\tau) = 0.27 \tag{S45}$$

$$\lim_{Re_\tau \to \infty} \kappa_g(Re_\tau) = 0.34, \tag{S46}$$

where the upper limit is close to 1/3 as advocated for in [15]. We expect that the rough wall κ_g should be identical to the smooth wall value, since roughness shifts the velocity profile without changing the slope. For the limited amount of rough wall points, it is difficult to discern if that is indeed the case.

The transition of κ_g at $Re_\tau \sim 10^4$ is consistent with the high Reynolds number transition region found previously [14, 16].

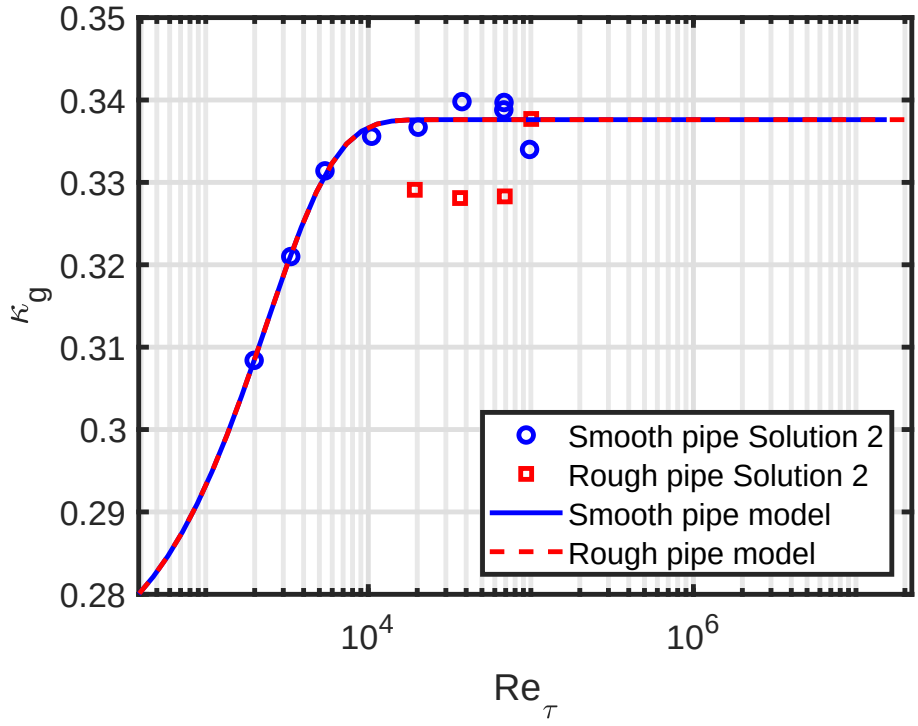

Figure S1: The global von Kármán number as a function of Re_τ. The models display Equation (S44). The smooth and rough pipe lines are identical and cannot be distinguished.

4.2. Local mixing lengths

The classical mixing length is derived from measurements in [17]:

$$\ell_{m,\mathrm{N}} = \delta \times \left[0.14 - 0.08\left(1-\frac{z}{\delta}\right)^2 - 0.06\left(1-\frac{z}{\delta}\right)^4\right] \tag{S47}$$

$$= \delta \times \left[0.4\left(\frac{z}{\delta}\right) - 0.44\left(\frac{z}{\delta}\right)^2 + 0.24\left(\frac{z}{\delta}\right)^3 - 0.06\left(\frac{z}{\delta}\right)^4\right], \tag{S48}$$

where we use the subscript "N" for Nikuradse.

Another mixing length can be derived from the log-law [18]:

$$\ell_{m,\mathrm{vK}} = \kappa_g \times z, \tag{S49}$$

where we use the subscript "vK" for von Kármán. This expression implies that the mixing length increases linearly from the wall with a slope κ_g.

Finally, a third mixing length is [19]:

$$\ell_{m,\mathrm{G-H}} = \delta \times \frac{\kappa_g}{6}\left[1-\left(1-\frac{z}{\delta}\right)^2\right]\left[1+2\left(1-\frac{z}{\delta}\right)^2\right] \tag{S50}$$

$$= \delta \times \kappa_g\left[\left(\frac{z}{\delta}\right)-\frac{11}{6}\left(\frac{z}{\delta}\right)^2+\frac{4}{3}\left(\frac{z}{\delta}\right)^3-\frac{2}{6}\left(\frac{z}{\delta}\right)^4\right], \tag{S51}$$

where we use the subscript "G-H" for Gersten-Herwig. All three normalised mixing length expressions are compared in Figure S2; since the von Kármán and Gersten-Herwig expressions are functions of κ_g, they vary (increase) with the friction Reynolds number, whereas the Nikuradse expression is independent of Re_τ.

For reference we have added the mixing length proposed in [20, 21] as a more recent example. This expression is quite similar to the Nikuradse mixing length and will not be used in the remainder of this SI.

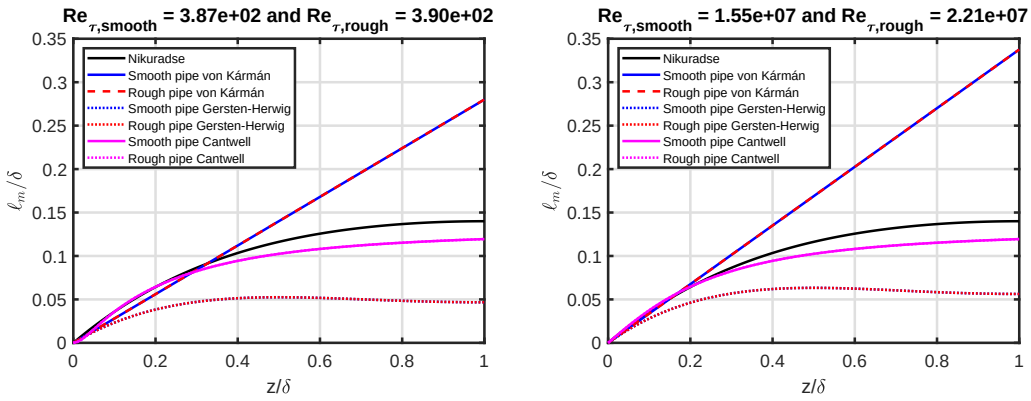

Figure S2: Normalised mixing length as a function of normalised pipe radius, left: Low friction Reynolds number, right: High friction Reynolds number. Smooth and rough pipe lines are almost identical and cannot be distinguished.

4.3. Centerline mixing lengths

The centerline (CL) value of the mixing length is the value on the pipe axis ($z/\delta = 1$). For the three mixing lengths considered, the CL values are:

$$\ell_{m,\mathrm{N,CL}} = 0.14 \times \delta \tag{S52}$$

$$\ell_{m,\mathrm{vK,CL}} = \kappa_g \times \delta \tag{S53}$$

$$\ell_{m,\mathrm{G-H,CL}} = \frac{\kappa_g}{6} \times \delta \tag{S54}$$

4.4. Area-averaged mixing lengths

The area-average (AA) of a quantity is defined as:

$$\langle \cdot \rangle_{\mathrm{AA}} = \frac{2}{\delta^2} \int_0^{\delta} [\cdot] \times (\delta - z) \mathrm{d}z \tag{S55}$$

$$= \frac{2}{Re_\tau} \int_0^{Re_\tau} [\cdot] \mathrm{d}z^+ - \frac{2}{Re_\tau^2} \int_0^{Re_\tau} [\cdot] \times z^+ \mathrm{d}z^+ \tag{S56}$$

Using this averaging on our three mixing lengths in Equations (S47), (S49) and (S50), we can write:

$$\langle \ell_{m,\mathrm{N}} \rangle_{\mathrm{AA}} = 0.08 \times \delta [22] \tag{S57}$$

$$\langle \ell_{m,\mathrm{vK}} \rangle_{\mathrm{AA}} = \frac{\kappa_g}{3} \times \delta [14] \tag{S58}$$

$$\langle \ell_{m,\mathrm{G-H}} \rangle_{\mathrm{AA}} = 0.14 \kappa_g \times \delta \tag{S59}$$

In Figure S3, we compare the three AA normalised mixing lengths as a function of Re_τ. As mentioned earlier, the Nikuradse mixing length is independent of Re_τ, whereas the von Kármán and Gersten-Herwig mixing lengths increase across the high Reynolds number transition region due to the increase of κ_g.

The CL-to-AA mixing length ratios are all constant:

$$\frac{\ell_{m,\mathrm{N,CL}}}{\langle \ell_{m,\mathrm{N}} \rangle_{\mathrm{AA}}} = 1.75 \tag{S60}$$

$$\frac{\ell_{m,\mathrm{vK,CL}}}{\langle \ell_{m,\mathrm{vK}} \rangle_{\mathrm{AA}}} = 3 \tag{S61}$$

$$\frac{\ell_{m,\mathrm{G-H,CL}}}{\langle \ell_{m,\mathrm{G-H}} \rangle_{\mathrm{AA}}} = 1.19 \tag{S62}$$

Using the AA formulation, we can also define the AA mean velocity as:

$$U_m = \langle U_{\mathrm{g,mean}} \rangle_{\mathrm{AA}} \tag{S63}$$

5. Turbulence Intensity

5.1. Friction factor

We introduce the friction factor λ through an equation relating it to the friction velocity and the AA mean velocity:

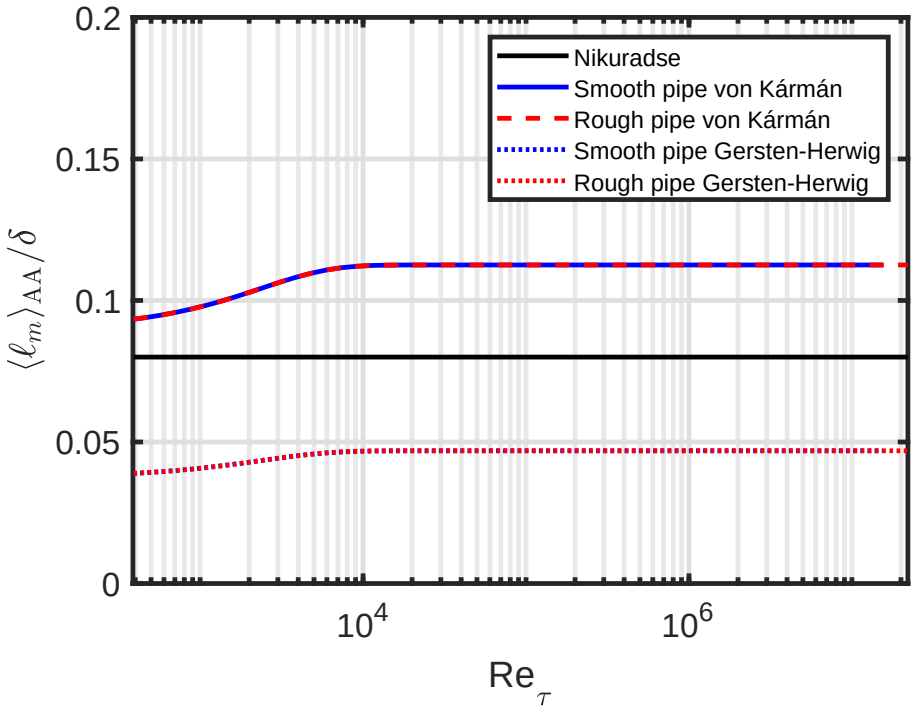

Figure S3: Area-averaged normalised mixing length as a function of the friction Reynolds number. Smooth and rough pipe lines are identical and cannot be distinguished.

$$u_\tau^2 = \frac{\lambda}{8} \times U_m^2, \tag{S64}$$

however, we note that this equation is not completely accurate for the measurements used, see [16].

5.2. TKE assumption

The TKE is equal to the sum of the contributions from streamwise, wall-normal and spanwise velocity fluctuations. We will assume that the TKE is proportional to the square of the streamwise velocity fluctuations:

$$k = \beta\overline{u^2} = \beta \times \frac{\overline{u^2}}{u_\tau^2} \times u_\tau^2 = \beta \times \frac{\overline{u^2}}{u_\tau^2} \times \frac{\lambda}{8} \times U_m^2, \tag{S65}$$

where β is a constant of proportionality.

5.3. Centerline

We can write the square of the normalised CL fluctuating velocity as [23]:

$$\frac{\overline{u^2_{\mathrm{CL}}}}{u^2_\tau} = B_g - \frac{C_g}{\sqrt{Re_\tau}}, \tag{S66}$$

which is shown in Figure S4 and observed to increase across the transition region.

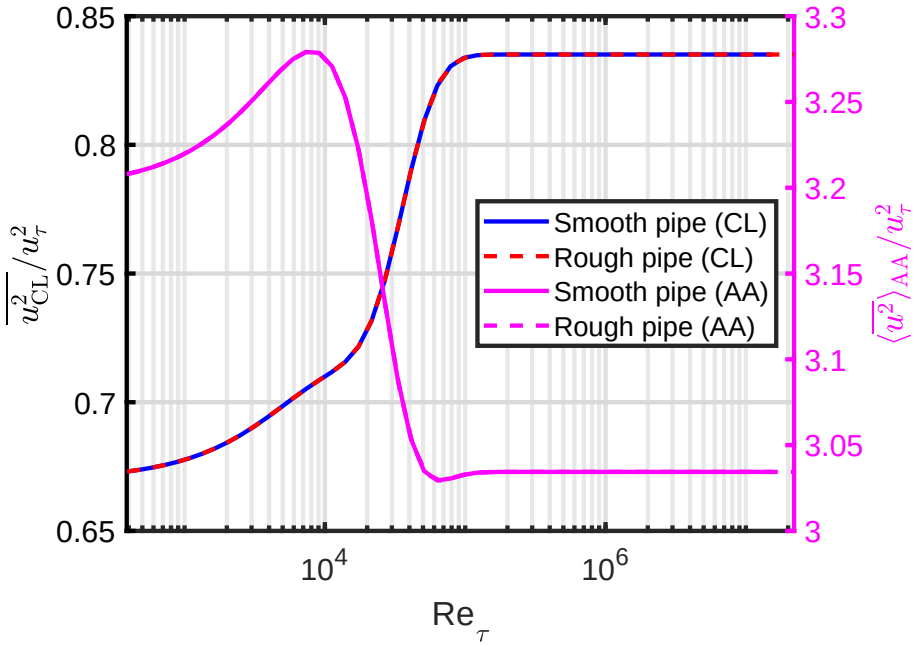

Figure S4: The square of the normalised CL and AA fluctuating velocity as a function of Re_τ. Smooth and rough pipe lines are identical and cannot be distinguished.

The square of the turbulence intensity (TI) at the CL is defined as:

$$I^2_{\mathrm{CL}} = \frac{\overline{u^2_{\mathrm{CL}}}}{U^2_{\mathrm{CL}}} = \frac{\overline{u^2_{\mathrm{CL}}}}{u^2_\tau} \times \frac{u^2_\tau}{U^2_{\mathrm{CL}}} \tag{S67}$$

$$= \left[B_g - \frac{C_g}{\sqrt{Re_\tau}}\right] \times \frac{u^2_\tau}{U^2_{\mathrm{CL}}}, \tag{S68}$$

where the mean CL velocity is related to the mean AA velocity as [24]:

$$U_{\mathrm{CL}} = 4.4441 \times u_\tau + U_m, \tag{S69}$$

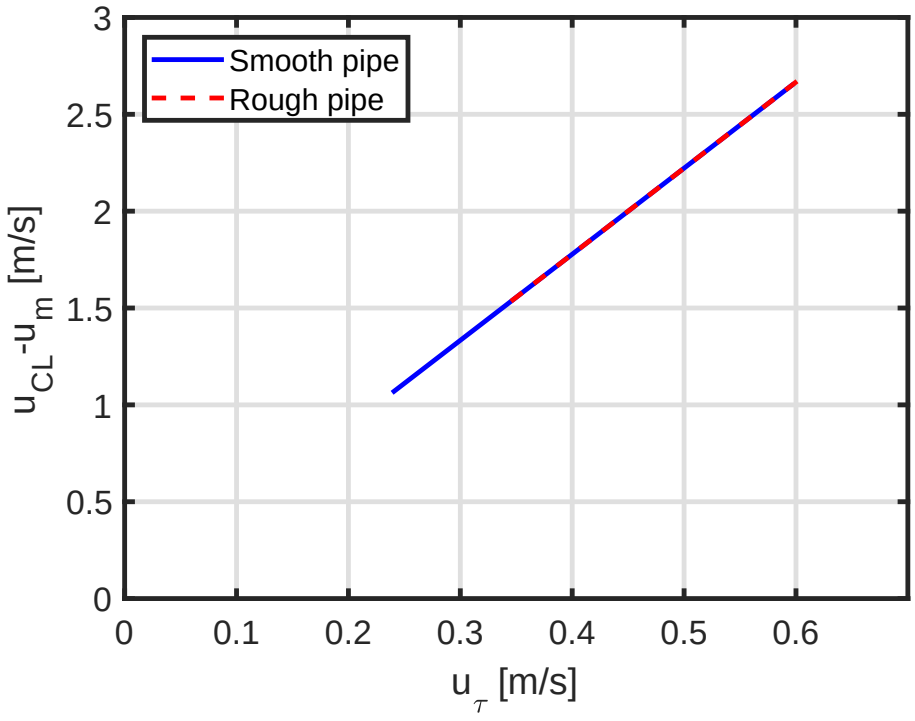

Figure S5: Difference between centerline and mean velocity as a function of friction velocity. Smooth and rough pipe values are on the same line.

see Figure S5.

Finally, the CL TKE is:

$$k_{\mathrm{CL}} = \beta U_{\mathrm{CL}}^2 I_{\mathrm{CL}}^2 = \beta \overline{u_{\mathrm{CL}}^2} \tag{S70}$$

$$= \beta \left[B_g - \frac{C_g}{\sqrt{Re_\tau}} \right] \times u_\tau^2 \tag{S71}$$

5.4. Area-averaged

We repeat our CL analysis above with the AA quantities; the square of the normalised AA fluctuating velocity is [16]:

$$\frac{\langle \overline{u^2} \rangle_{\mathrm{AA}}}{u_\tau^2} = B_g + \frac{3}{2} A_g - \frac{8 C_g}{3\sqrt{Re_\tau}}, \tag{S72}$$

see Figure S4. Overall the trend for higher Reynolds number is a decrease as opposed to the CL behaviour, but it has a peak value before beginning the reduction towards higher Reynolds numbers.

The square of the AA TI is defined as:

$$I^2_{\mathrm{AA}} = \frac{\langle\overline{u^2}\rangle_{\mathrm{AA}}}{U_m^2} = \frac{\langle\overline{u^2}\rangle_{\mathrm{AA}}}{u_\tau^2} \times \frac{u_\tau^2}{U_m^2} = \frac{\langle\overline{u^2}\rangle_{\mathrm{AA}}}{u_\tau^2} \times \frac{\lambda}{8} \tag{S73}$$

$$= \left[B_g + \frac{3}{2}A_g - \frac{8C_g}{3\sqrt{Re_\tau}}\right] \times \frac{\lambda}{8}, \tag{S74}$$

with a corresponding AA TKE:

$$k_{\mathrm{AA}} = \beta U_m^2 I^2_{\mathrm{AA}} = \beta\langle\overline{u^2}\rangle_{\mathrm{AA}} \tag{S75}$$

$$= \beta\left[B_g + \frac{3}{2}A_g - \frac{8C_g}{3\sqrt{Re_\tau}}\right] \times \frac{\lambda}{8} \times U_m^2 \tag{S76}$$

5.5. Mixed

For reference, we include what we call the mixed TI definition from [13], which consists of a combination of CL and AA quantities [25]:

$$I^2_{\mathrm{mix}} = \frac{\overline{u^2_{\mathrm{CL}}}}{U_m^2} = \frac{\overline{u^2_{\mathrm{CL}}}}{u_\tau^2} \times \frac{u_\tau^2}{U_m^2} = \frac{\overline{u^2_{\mathrm{CL}}}}{u_\tau^2} \times \frac{\lambda}{8} \tag{S77}$$

$$= \left[B_g - \frac{C_g}{\sqrt{Re_\tau}}\right] \times \frac{\lambda}{8}, \tag{S78}$$

with a corresponding mixed TKE:

$$k_{\mathrm{mix}} = \beta U_m^2 I^2_{\mathrm{mix}} = \beta\overline{u^2_{\mathrm{CL}}} \tag{S79}$$

$$= \beta\left[B_g - \frac{C_g}{\sqrt{Re_\tau}}\right] \times \frac{\lambda}{8} \times U_m^2 \tag{S80}$$

6. Model input

The Princeton Superpipe parameters used are taken from [26]. The pipe diameters for smooth and rough pipes are:

$$D_{\mathrm{smooth}} = 2 \times 64.68 \text{ mm} \tag{S81}$$

$$D_{\mathrm{rough}} = 2 \times 64.92 \text{ mm} \tag{S82}$$

For the experiments, the mean velocity was held close to constant; we use this value, which is close to the ones measured:

$$U_m = 10 \text{ m/s} \tag{S83}$$

The Reynolds number was mainly changed by varying the air pressure; we use a range of kinematic viscosities extending beyond the measured Reynolds numbers:

$$\nu_{\text{kin}} = [10^{-9}, 10^{-4}] \text{ m}^2/\text{s} \tag{S84}$$

For the rough pipe, we use the sand-grain roughness [24]:

$$k_s = 3 \ \mu\text{m} \tag{S85}$$

The pipe diameter, mean velocity and kinematic viscosity are used to define the bulk Reynolds number:

$$Re_D = \frac{DU_m}{\nu_{\text{kin}}} \tag{S86}$$

7. Model assumptions

For the equilibrium assumption, the Reynolds stress is related to the friction velocity as [3]:

$$-\overline{uv}_{\text{P}} = u_\tau^2 \tag{S87}$$

Adapting this to non-equilibrium flows using Equation (S19) we get:

$$-\overline{uv}_{\text{K}-\text{P}} = u_\tau^2 \left(\frac{\mathcal{P}}{\varepsilon}\right)^{-1/2} \tag{S88}$$

Differentiating the log-law with respect to z, the mean shear rate can be expressed as:

$$\mathcal{S} = \frac{u_\tau}{\ell_m}, \tag{S89}$$

where ℓ_m is the von Kármán mixing length as given in Equation (S49). Although inconsistent, we will assume that the mean shear rate can be expressed using the above equation even for the other two mixing lengths treated.

We will not assume equilibrium flows, so we explicitly write:

$$\frac{|\overline{uv}|}{k} \neq 0.3, \tag{S90}$$

and:

$$\mathcal{P} \neq \varepsilon \tag{S91}$$

8. Model choices

Since we only have the AA turbulence production-to-dissipation ratio, we use AA for all other quantities as well to ensure consistency.

AA length scales can be used to define an AA mean shear rate:

$$\mathcal{S}_{\mathrm{AA}} = \frac{u_\tau}{\langle \ell_m \rangle_{\mathrm{AA}}}, \tag{S92}$$

see Figure S6. We will use the Gersten-Herwig mixing length $\langle \ell_{m,\mathrm{G-H}} \rangle_{\mathrm{AA}}$, since it includes a κ_g-dependency, has been compared to measurements and possesses the correct overall behaviour of a linear rise from the wall which develops to a constant towards the CL. However, it is only roughly half of the Nikuradse length scale; it is not clear to us why there is such a large difference.

We note that the log-law leads to a single length scale [14], whereas the velocity fluctuations lead to two length scales as discussed in [16].

The friction velocity from [1] can be used to calculate the relationship between the friction and bulk Reynolds numbers:

$$Re_\tau = \frac{Ru_\tau}{\nu_{\mathrm{kin}}} = \frac{u_\tau}{2U_m} \times Re_D, \tag{S93}$$

see Figure S7.

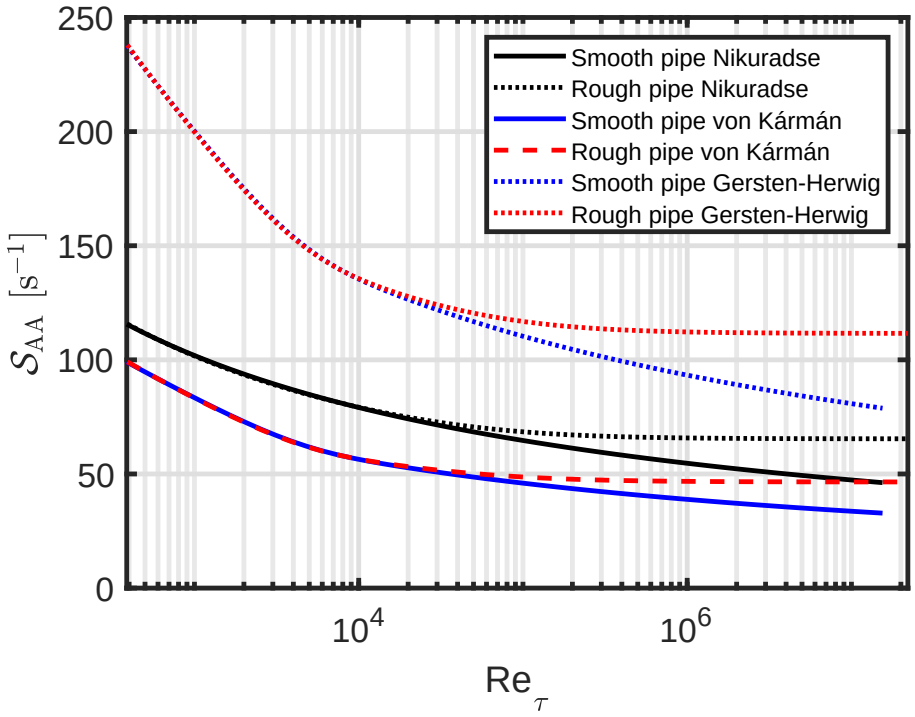

Figure S6: The AA mean shear rate as a function of Re_τ with length scales from Figure S3 and friction velocities from [1].

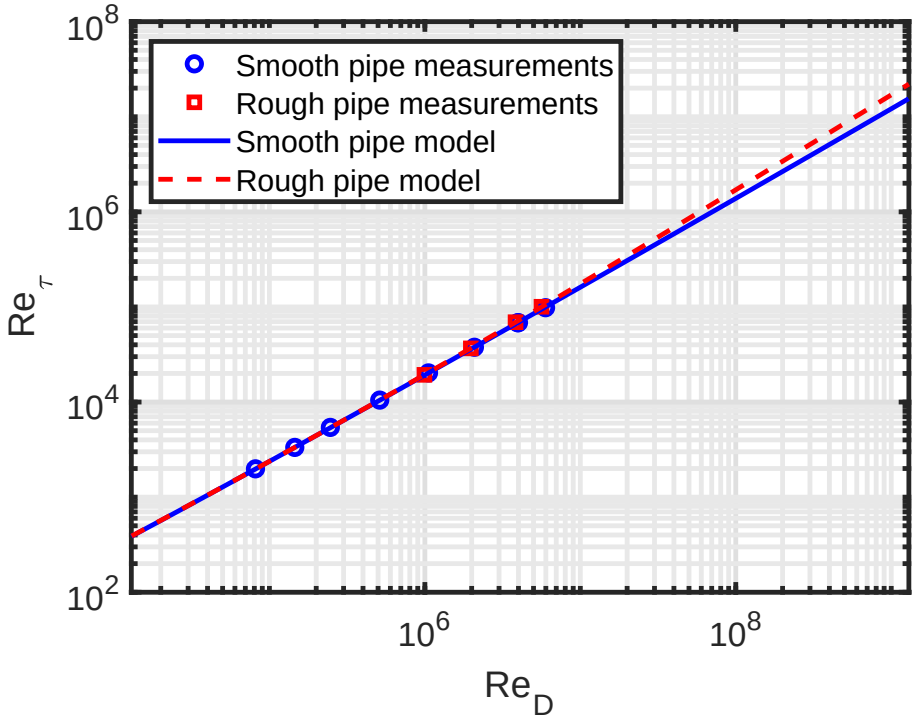

Figure S7: Friction Reynolds number as a function of bulk Reynolds number. Superpipe measurements are included.

References

[1] Basse NT. An algebraic non-equilibrium turbulence model of the high Reynolds number transition region (2023).

[2] Pope SB. Turbulent Flows. *Cambridge University Press* **2000**.

[3] Apsley DD. Turbulence modelling. [Online]
`https://personalpages.manchester.ac.uk/staff/david.d.apsley/lectures/comphydr/index.htm`
(accessed September 2023)

[4] Boussinesq J. Essai sur la théorie des eaux courantes. Mémoires présentés par divers savants á l'Académie des Sciences **23**, 1-680 (1877).

[5] Prandtl L. Bericht über Untersuchungen zur ausgebildeten Turbulenz. Z. Angew. Math. Mech. **5**, 136–139 (1925).

[6] Prandtl L. Bericht über neuere Turbulenzforschung, in: Hydraulische Probleme. *VDI-Verlag, Berlin* **1926**.

[7] Kolmogorov AN. The equations of turbulent motion in an incompressible fluid (in Russian). Izvestia Acad. Sci., USSR; Phys. **6**, 56-58 (1942).

[8] Prandtl L. Über ein neues Formelsystem für die ausgebildete Turbulenz. Nachr. Akad. Wiss. Göttingen Math.-Phys. Klasse, 6-19 (1945).

[9] Taylor GI. Statistical theory of turbulence, Parts I-IV. Proc. R. Soc. Lond. A **151**, 421-478 (1935).

[10] Wilcox DC. Turbulence Modeling for CFD, Third Edition. *DCW Industries* **2006**.

[11] Jones WP and Launder BE. The prediction of laminarization with a two-equation model of turbulence. Int. J. Heat Mass Transfer **15**, 301-314 (1972).

[12] Bradshaw P, Ferriss DH and Atwell NP. Calculation of boundary-layer development using the turbulent energy equation. J. Fluid Mech. **28**, 593-616 (1967).

[13] Ansys Fluent User's Guide, Release 2022 R2 (2022).

[14] Basse NT. Scaling of global properties of fluctuating and mean streamwise velocities in pipe flow: Characterization of a high Reynolds number transition region. Phys. Fluids **33**, 065127 (2021).

[15] Tennekes H and Lumley JL. A First Course in Turbulence. *MIT Press* **1972**.

[16] Basse NT. Scaling of global properties of fluctuating streamwise velocities in pipe flow: Impact of the viscous term. Phys. Fluids **33**, 125109 (2021).

[17] Nikuradse J. Gesetzmäßigkeiten der turbulenten Strömung in Glatten Rohren. VDI Forschungsheft **356**, 1-36 (1932).

[18] Kármán Th. von. Mechanische Ähnlichkeit und Turbulenz. Nachrichten von der Gesellschaft der Wissenschaften zu Göttingen, Mathematisch-Physikalische Klasse **1930**, 58-76 (1930).

[19] Gersten K and Herwig H. Strömungsmechanik. *Springer* **1992**.

[20] Cantwell BJ. A universal velocity profile for smooth wall pipe flow. J. Fluid Mech. **878**, 834-874 (2019).

[21] Cantwell BJ, Bilgin E and Needels JT. A new boundary layer integral method based on the universal velocity profile. Phys. Fluids **34**, 075130 (2022).

[22] Greenshields C. Private Communication (2021).

[23] Basse NT. Extrapolation of turbulence intensity scaling to $Re_\tau \gg 10^5$. Phys. Fluids **34**, 075128 (2022).

[24] Basse NT. Turbulence intensity scaling: A fugue. Fluids **4**, 180 (2019).

[25] Basse NT. Mind the gap: Boundary conditions for turbulence modelling. [Online]
`https://www.researchgate.net/publication/359218404_Mind_the_Gap_Boundary_Conditions_for_Turbulence_Modelling`
(accessed September 2023)

[26] Hultmark M, Vallikivi M, Bailey SCC and Smits AJ. Logarithmic scaling of turbulence in smooth- and rough-wall pipe flow. J. Fluid Mech. **728**, 376-395 (2013).